

# Synthesis and Oxygen-Permeation Properties of Thin YSZ/Pd Composite Membranes

Jinsoo Kim and Y. S. Lin

Dept. of Chemical Engineering, University of Cincinnati, Cincinnati, OH 45221

*Thin dense yttria-stabilized-zirconia (YSZ)/Pd composite (dual-phase) membranes were fabricated on porous YSZ membranes by a new approach that combines the reservoir method and chemical vapor deposition (CVD) technique. A thin porous YSZ layer was coated on a porous alumina support by dip coating the YSZ suspension. A continuous Pd phase was formed inside pores of the YSZ layer by the reservoir method. The residual pores of the YSZ/Pd layer were plugged with yttria/zirconia by CVD to ensure the gas tightness of the membranes. The oxygen-permeation fluxes through these composite (dual-phase) membranes, measured in situ in the CVD reactor, are  $2.0 \times 10^{-8}$  and  $4.8 \times 10^{-8}$  mol/cm<sup>2</sup>·s at 1,050°C when air and oxygen are used as the permeate gases, respectively. These oxygen-permeation values are about 1 order of magnitude higher than those of pure YSZ membranes prepared under similar conditions. The apparent activation energies for oxygen permeation at 900–1,050°C are 193 kJ/mol for thin YSZ/Pd composite (dual-phase) membranes and 124 kJ/mol for pure YSZ membranes. These results are explained in terms of relative importance of various mass-transfer steps for oxygen permeation and microstructure of the YSZ/Pd composite membranes prepared by this technique.*

## Introduction

In recent years, mixed-conducting inorganic membranes, in which both ionic and electronic charge carriers exist, have received increasing attention because of their potential applications ranging from small-scale oxygen pumps for medical applications to large-scale combustion processes such as coal liquefaction. Among mixed-conducting inorganic membranes, dense perovskite membranes are well known because of their high oxygen permeability at elevated temperatures when subjected to a gradient of oxygen chemical potential (Bouwmeester et al., 1994; Zeng et al., 1998). Although they have shown good performances in a lot of technological applications, they have some limitations when used in harsh conditions such as highly reducing atmosphere because of their chemical stability problems (Pei et al., 1995).

Another group of dense inorganic membranes is based on the fast oxygen ionic conductors (electrolytes). Well-known electrolytes are yttria stabilized zirconia (YSZ) and bismuth-based oxides. Especially, YSZ has a very good chemical,

structural, and phase stability. Its cubic-fluorite structure is stable between room temperature and 3000 K. However, the oxygen permeation flux through these membranes is relatively low because of the large transport resistance caused by the low electronic conductivity and/or large thickness of the membranes prepared by conventional preparation methods.

Two different approaches can be employed on the development of high oxygen semipermeable inorganic membranes with minimized transport resistance: (1) increasing the electronic conductivity, and (2) reducing the membrane thickness. Some research groups have attempted to improve the electronic conductivity of the fast oxygen ionic conducting materials by various methods. Most work has been conducted on doping various multiple valent cations into fast ionic conducting materials to establish good electronic conductivity (such as ZrO<sub>2</sub>-CeO<sub>2</sub>-Y<sub>2</sub>O<sub>3</sub> (Nigara et al., 1995), ZrO<sub>2</sub>-TiO<sub>2</sub>-Y<sub>2</sub>O<sub>3</sub> (Arashi and Naito, 1992), ZrO<sub>2</sub>-TbO<sub>2</sub>-Y<sub>2</sub>O<sub>3</sub> (Han and Worrell, 1995)). Also, some research groups have investigated the reduction of the membrane thickness with various techniques such as the chemical/electrochemical vapor deposition (CVD/EVD) (Lin et al., 1992; Brinkman et al., 1994;

Correspondence concerning this article should be addressed to Y. S. Lin.

Han et al., 1997), and the physical sputtering method (Wang and Barnett, 1993; Jankowski and Hayes, 1995). Membranes prepared by both methods showed improvement of oxygen permeation flux to some extent.

Recently, dual-phase composite materials with much improved conducting properties have been studied and used as membranes for oxygen separation (Mazanec et al., 1992; Shen et al., 1994; Chen et al., 1995, 1996). The concept of dual-phase membranes was first introduced by Mazanec et al. (1992). They made the composites of YSZ and Pd (or including In/Pr), and showed much improved oxygen permeation flux when the metal volume was above the percolation threshold (the volume that makes the metal phase continuous). After that, several researchers reported improved oxygen permeation fluxes with different sets of materials. Chen et al. (1995, 1996) reported YSZ/Pd, bismuth oxide-erbium (BE)/Ag, and BE/Au-based dual-phase membranes. Bismuth oxide-yttria (BY)/Ag dual-phase composites were reported by Shen et al., (1994).

Membranes made from these composite materials consist of two phases: one phase with high oxygen ionic conductivity, and the other with high electronic conductivity, as shown in Figure 1a. These dual-phase membranes showed much improved oxygen permeation flux, when both phases became continuous. The oxygen permeation flux of these dual-phase membranes is close to the mixed electronic and oxygen ionic conducting perovskite materials, which have been known as one of the most oxygen permeable materials at elevated temperatures. All the reported dual-phase membranes were prepared by the method of solid-state powder pressing and sintering. The thickness was in the 0.25–2 mm range.

Preparation of thin dual-phase membranes supported on porous ceramic substrates is highly desirable, as these thin dual-phase membranes offer not only a higher oxygen permeation flux but also a substantial saving in the use of the expensive membrane materials. In this article, we report a new concept of thin dual-phase membranes and the results of our efforts to prepare such membranes by a new approach that combines liquid-phase and vapor-phase deposition methods.

## Experimental

### Thin dual-phase membrane

The thin dual-phase membrane consists of a porous alumina support and thin dual phase layer of metal and oxygen ionic conductor, as shown in Figure 1b. In this study, palladium and yttria-stabilized zirconia (YSZ) were selected as the metal and ionic conducting ceramic phases. While the bulk dual-phase membranes have a thickness of 0.25–2 mm, this thin dual-phase membrane will have a thickness of less than 10  $\mu\text{m}$ . Since it is difficult to prepare such thin dual-phase layers on the porous ceramic supports by the conventional method, in this study the thin dual-phase layers were prepared by an approach combining the liquid and vapor coating methods.

First, a porous, 10- $\mu\text{m}$ -thick, YSZ layer was coated on a porous  $\alpha$ -alumina support by the suspension/slip-casting coating method. Then a continuous Pd phase was coated inside the pores of the porous YSZ layer by impregnation. Finally, the residual pores of Pd-modified YSZ membranes were

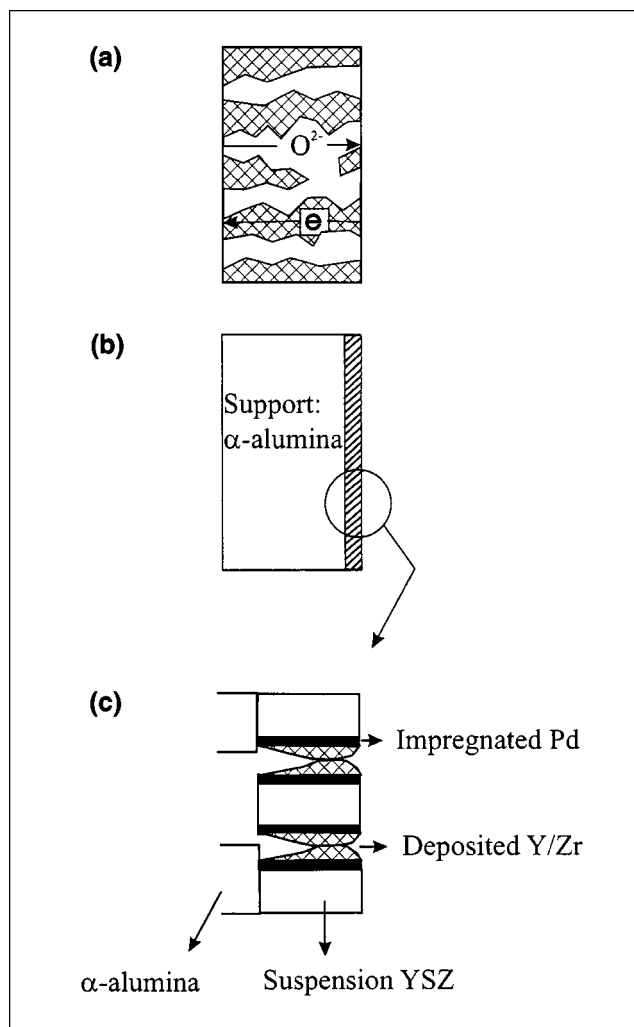


Figure 1. (a) Symmetric dual-phase membrane (conventional membrane), (b) thin composite (dual-phase) membrane, and (c) its structure (new membrane).

plugged by yttria/zirconia (YZ) by a counterdiffusion chemical vapor deposition (CVD) technique. The membrane prepared by these procedures would ideally give a structure shown in Figure 1c. It has continuous phases of YSZ (formed by suspension coating and CVD) and Pd (formed by wet impregnation). The detailed procedures are described next.

### Synthesis of Pd-impregnated YSZ membranes

Stable YSZ suspension was prepared from commercially available YSZ powder (Tosho, TZ-8Y). The YSZ powder and dilute nitric acid were mixed together in a polyethylene bottle by the weight ratio of 1:2. Different pH values of nitric acid were tried to find appropriate values for stable YSZ suspension. After adding YSZ milling balls (1mm diameter), the mixture was ball-milled for 7 days. After rolling, the suspension was ultrasonically treated to break the agglomerates. Polyvinyl alcohol (PVA) was used in the present work as a drying control chemical additive (DCCA). PVA solution was

prepared by dissolving 3 g of PVA (Fluka, MW = 72,000) in 95 mL water and 5 ml of 1 M HNO<sub>3</sub> solution. Before a membrane layer was made from the suspension, the PVA solution in a volume ratio of 25% was added to the suspension to prevent crack formation during the drying process.

The supported YSZ membranes were prepared by dip-coating the YSZ suspension on the homemade  $\alpha$ -alumina disks (diameter: 20 mm; thickness: 2 mm; pore diameter: 0.2  $\mu$ m; porosity: 50%). The thickness of the supported YSZ membrane was controlled by the number of dip-coatings. The supported suspension-derived YSZ membranes were dried at a relative humidity of 40–50% and temperature of 40°C. Then, they were sintered at 1,000°C for 3 h.

The pores of YSZ membranes were modified with Pd by the reservoir method (Uhlhorn et al., 1992). First, a Pd solution was prepared by dissolving 0.25 g of Pd acetate (Alfa, MW = 673.46) in a mixture of 0.3 mL of HCl and 10 mL of acetone. The prepared supported YSZ membranes were soaked in the Pd solution for 30 min to fully saturate both the  $\alpha$ -alumina support and the porous YSZ top layer. After that, they were taken out and dried in the hood for 1 day. During the drying process, the membranes were placed on a nonporous plate with the YSZ top layer facing upwards. The dried Pd-impregnated YSZ membranes were calcined at 500°C for 2 h under hydrogen flow at a heating/cooling rate of 4°C/min. These soaking, drying, and calcination processes were repeated to get an appropriate amount of Pd inside the porous YSZ membranes.

## Membrane preparation

Thin YSZ/Pd composite (dual-phase) membranes were prepared by plugging the residual pores of Pd-impregnated YSZ membranes by CVD, in a homemade CVD reactor. The CVD reactor, presented in Figure 2, consisted of three parts: a reactor part, a temperature-control part, and a pressure-control part. The reactor part was made of two dense alumina tubes. The larger tube (length: 50 in., 1.3m; OD: 2 in., 51 mm) was used as a metal source chamber, and the smaller one (length: 15 in. 0.4 m; OD: 1 in., 25 mm) as an oxygen source chamber. The temperature and pressure inside the reactor were controlled by two tubular furnaces (ThermoLyne) and a pressure-control system, consisting of vacuum pumps (GE Motors), pressure sensors (MKS), and control valves (MKS).

CVD experimental conditions are presented in Table 1. In the CVD experiment, the porous Pd-modified YSZ membrane was sealed on top of the smaller alumina tube that separated the oxygen chamber and the metal precursor chamber. The metal precursors, ZrCl<sub>4</sub> and YCl<sub>3</sub> (Strem), were placed at the desired temperature zone, which was selected based on the equilibrium vapor pressure data (Barin, 1995; Barin and Knacke, 1973). Sublimation temperatures for ZrCl<sub>4</sub> and YCl<sub>3</sub> were fixed at 190°C and 700°C, respectively. After placing the substrate and precursors, the reactor was evacuated and heated slowly to the desired temperature under the flow of Ar (with 1% of H<sub>2</sub>) to the metal source chamber. At the time when reactor pressure and temperature were stabilized, the CVD experiment was started by introducing

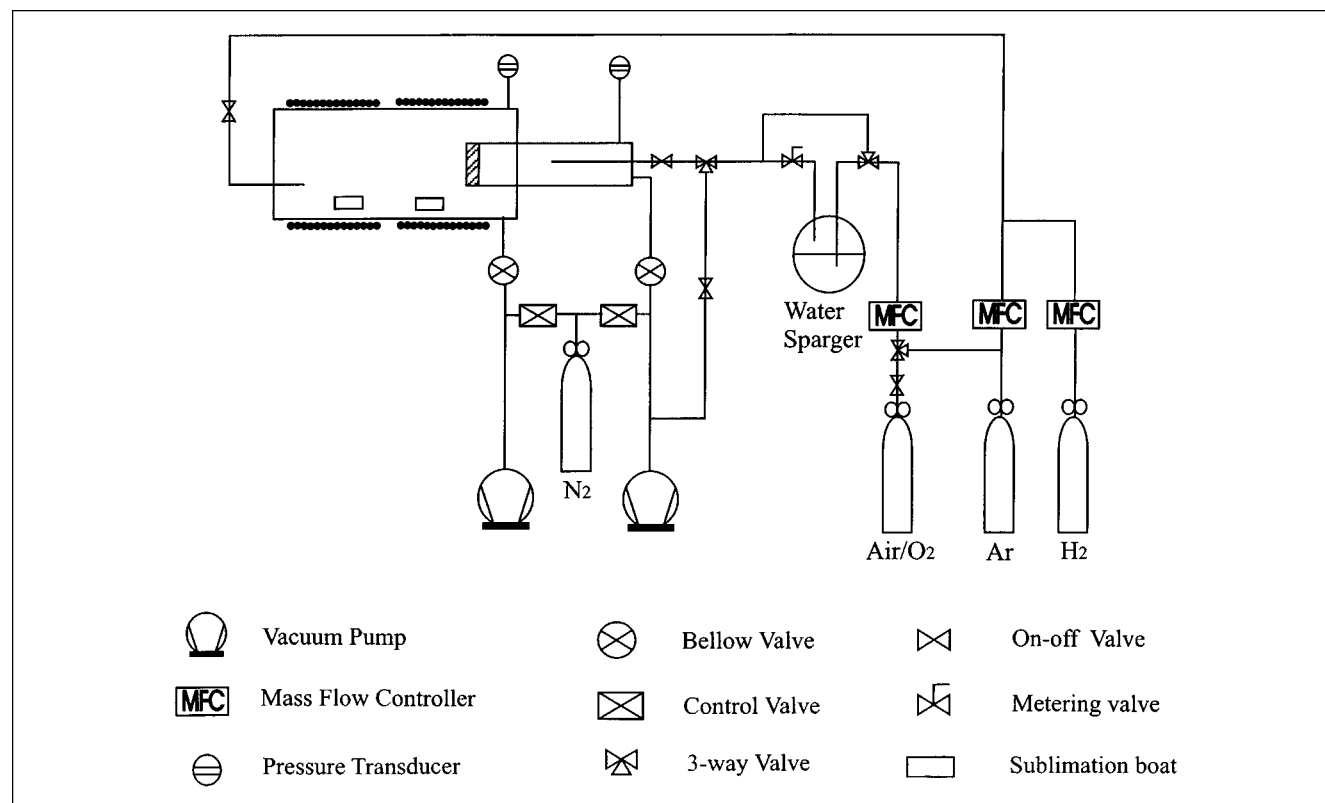


Figure 2. CVD reactor.

**Table 1. Experimental Conditions for CVD and *in situ* Oxygen Permeation**

Chemical Vapor Deposition	
Deposition temperature	1,000°C
Reactor pressure	10–15 torr
Gas flow rate in metal source chamber	Ar = 9.9 mL/min H <sub>2</sub> = 0.1 mL/min
Air flow rate in oxygen source chamber	5 mL/min
ZrCl <sub>4</sub> temperature	190°C
YCl <sub>3</sub> temperature	700°C
<i>In-Situ</i> Oxygen Permeation	
Reactor temperature	900–1,050°C
Pressure in metal source chamber	< 10 torr
Pressure in oxygen source chamber	50 torr

the oxygen-source stream into the CVD reactor. Simultaneously, the Ar flow to the oxygen-source chamber was stopped. After the desired deposition time was reached, the CVD process was terminated by switching off the flow of the oxygen-source precursor, followed by flushing with Ar.

### **Membrane characterization and oxygen permeation experiments**

The presence of palladium inside porous YSZ membranes and the crystal phase structure of YSZ/Pd composite (dual-phase) membranes were analyzed by an X-ray diffractometer (Siemens, CuK $\alpha$  radiation). The crystallite sizes of YSZ and Pd were calculated from the XRD line broadening by the Scherrer's equation (Cullity, 1978). The electrical conductivity of the Pd-modified YSZ membranes was examined with a four-point DC method (Qi and Lin, 1999). The thickness of the deposited films was estimated from a scanning electron microscope (Hitachi) picture of the cross section of the membranes.

Gas-permeation experiments were performed in the CVD reactor to check the gas tightness and measure the oxygen-permeation flux through the CVD-prepared thin YSZ/Pd composite (dual-phase) membranes. Since the CVD process is a self-plugging process, *in situ* gas-permeation experiments can avoid the high-temperature sealing problem and other difficulties associated with measuring gas permeation through these membrane composites using a special permeation apparatus (Lin et al., 1992). The extent of substrate pore modification was roughly checked by an Ar-permeation test at the deposition temperature with progression of the CVD experiment. After deposition, Ar- and N<sub>2</sub>-permeation experiments were performed before measuring the oxygen-permeation flux to estimate the leakage through the membrane and/or sealing defects. Air and pure oxygen were used as permeate gases in the oxygen permeation experiments.

Before gas-permeation experiments, the temperatures of the sublimation beds were reduced (< 400°C for YCl<sub>3</sub> and < 100°C for ZrCl<sub>4</sub>) to minimize CVD film growth during this stage. A gas-permeation experiment was prepared by flushing the oxygen source chamber with a permeate gas, while the Ar stream containing 1% H<sub>2</sub> (as an oxygen getter) flowed through the metal source chamber at about 3 torr total pressure. After about 30 min flushing, the pressure of the oxygen source chamber was increased by introducing a permeate gas. The

precursor chamber was maintained in vacuum. When the pressure of the oxygen source chamber was stabilized at 50 torr, the oxygen source chamber was isolated by closing all the inlet and outlet valves connected to the chamber. The total pressure of the oxygen source chamber was measured as a function of time. The slopes of the pressure vs. time data were used to calculate the permeation flux of the permeate gas. The experimental conditions for the *in situ* gas-permeation experiments are also summarized in Table 1.

## **Results and Discussion**

### **Membrane characteristics**

A stable YSZ suspension was prepared by ball-milling the commercially available YSZ powder (Tosoh). The particle sizes of the powder were measured by SEM before and after the ball-milling process. The Tosoh's YSZ powder is made of large spherical aggregates with a wide size distribution (0.2–10  $\mu$ m). After 7 days of ball-milling, the YSZ particle size was in the range of 50–100 nm. The YSZ crystallite size, as suggested by the supplier (Tosoh), is 26 nm. Apparently, the YSZ particles in the suspension contain many small YSZ crystallites. By settling experiments, the optimum pH value was found to be 3–4 for the stable YSZ suspension.

Crack-free supported YSZ membranes could be prepared by dip-coating the stable YSZ suspension on  $\alpha$ -alumina supports. The YSZ layer thickness was about 5  $\mu$ m after 1-time dip-coating and 10  $\mu$ m after 2-time dip-coating, respectively. The average pore diameter of YSZ membranes was 100 nm when measured by a mercury porosimeter, and 114 nm estimated by the helium permeation method. More detailed results on the YSZ membranes were reported elsewhere (Kim and Lin, 1999).

The prepared porous YSZ membranes were modified with Pd by the reservoir method. The  $\alpha$ -alumina/YSZ two-layer membranes were put in the Pd solution, followed by drying, which promoted the concentration of the metal cations inside the top layer of the membranes. The thin YSZ top layer had a smaller pore size compared to the thick alumina support layer. During the drying process, the evaporation begins from the top layer. Because the Pd solution in the YSZ layer was dried, the impregnated solution inside the alumina layer filled the pores of the YSZ top layer by the capillary pressure that resulted from the difference in the pore sizes. During the calcination, the Pd precursor changed into pure Pd.

The XRD patterns of the Pd-modified YSZ membranes show two distinctive phases of YSZ and Pd. This indicates that all the Pd solution was completely changed into pure metal Pd during the calcination step. The electrical conductivity of the Pd-modified YSZ membranes is presented with the number of Pd impregnation in Figure 3. Since the four-point DC method measures the total conductivity, the conductivity shown in Figure 3 is dominated by the larger one of the electronic or ionic conductivity.

The conductivity of pure YSZ and 3-time Pd impregnated YSZ membranes is due to the oxygen ionic conductivity of YSZ phase, with an activation energy of about 86 kJ/mol. These are consistent with the data in the literature (Park and Blumenthal, 1989). The electronic conductivity of YSZ is in the range of about 10<sup>-4</sup>–10<sup>-6</sup> S/cm, several orders of magnitude lower than its oxygen ionic conductivity under the same

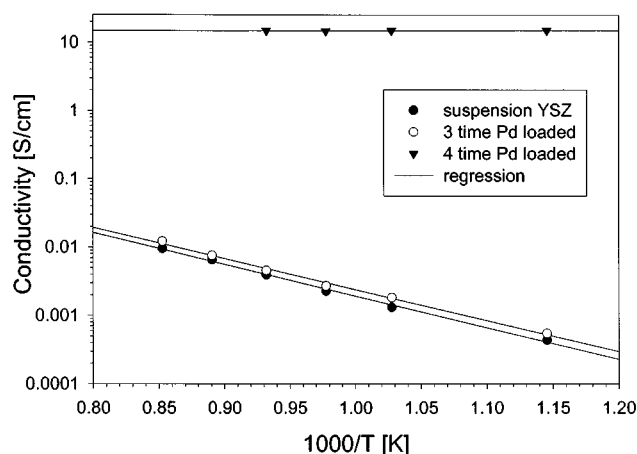


Figure 3. Electrical conductivity with the number of Pd impregnation.

conditions (Park and Blumenthal, 1989). Thus, the contribution of electron conduction to the total conductivity in these two YSZ membranes is negligible. These show that Pd after 3-time impregnation did not form a continuous phase. However, the total electrical conductivity of the 4-time Pd impregnated YSZ membrane is three orders of magnitude higher than that of the two membranes, as shown in Figure 3. This indicates that the Pd phase became continuous after 4-time impregnation, and the measured conductivity is that of metallic palladium. Based on these results, the 4-time Pd-impregnated YSZ membranes were used as the substrates for CVD experiments.

Yttria/zirconia (YZ) was deposited inside and/or on top of the Pd-impregnated YSZ membranes by the CVD process to prepare thin YSZ/Pd composite (dual-phase) membranes. The unique feature of the counter diffusion CVD process is the formation of the YZ deposit inside the pores of the Pd-impregnated YSZ membranes, in contrast to other deposition techniques that result in the formation of a film on the substrate surface. The progress of the CVD stage results in significant pore narrowing until all the pores are completely closed. After this pore closure, direct contact of the precursors is no longer possible.

However, film growth may continue since the oxygen precursor permeates through the YZ deposit or YSZ and meets metal precursors at the opposite side of the film, resulting in further reactions and solid film growth.

Figure 4 shows *in situ* Ar gas permeability with time during the CVD stage. After each 5 min of deposition, the CVD process was halted by switching off the supply of oxygen precursor, and *in situ* Ar gas permeation measurement was conducted. The decrease of the Ar gas permeability with deposition time indicates YZ deposition in the pores of the substrate, resulting in pore narrowing with the deposition. From Figure 4, the pore closure time was determined to be 20–25 min. *In situ* permeation experiments were tried just after pore closure. However, these membranes could not maintain the gas tightness for a sufficiently long time to complete the gas-permeation experiments. Therefore, additional deposition was carried out to increase the YZ plug thickness inside the pores so as to ensure the gas tightness of the membranes.

Figure 5 shows SEM secondary electron (SE) image and EDS dot mappings of Al, Pd, and Zr of the cross section of one of such membranes. Figure 5a and 5b indicate clearly a 10- $\mu$ m YSZ layer on the porous alumina support. Some zirconia appears to have penetrated into the alumina support, as shown in Figure 5c. A small amount of zirconia could penetrate into the support during both slip-casting and CVD processes. EDS dot mapping of Pd shows that palladium is concentrated inside the YSZ layer, leaving some Pd traces in the  $\alpha$ -alumina support. It also shows a fairly uniform distribution of palladium in the YSZ top layer, indicating the effectiveness of loading Pd uniformly on the top layer by the reservoir method.

Figure 6 is one typical XRD pattern of the YSZ/Pd thin dual-phase membranes prepared in this work. The YSZ peaks in the XRD pattern show that this CVD-prepared YSZ film has a cubic phase. Also, Pd peaks at the two theta values of 40 and 47 degrees indicate the presence of pure metal Pd, well crystallized in the standard face-centered cubic (fcc) system. It is interesting to note that no XRD peaks of PdO were observed on these membranes. This indicates that palladium was not oxidized during CVD and subsequent oxygen permeation experiments at high temperatures. The unlabeled small peaks are from the alumina support.

The thickness of dense YSZ formed by CVD was roughly measured by SEM observation of the membrane cross section. The XRD intensity ratio  $R [= I_{\text{Pd}(111)}/I_{\text{YSZ}(111)}]$ , compared to that of Pd-impregnated YSZ membranes, also represents the extent of YSZ deposit by CVD. A smaller value of  $R$  indicates thicker YSZ deposited by CVD on the porous YSZ/Pd support. The film thickness and the XRD intensity ratio of  $R$  for the YSZ/Pd membranes with different CVD deposition time is given in Table 2. As shown, the thickness of the dense YSZ film increases from 0.4  $\mu$ m to 3  $\mu$ m with CVD time increasing from 15 min to 80 min. The membranes that showed gas tightness for a prolonged time during oxygen permeation experiments had the dense YSZ layer of thickness about 2 to 3  $\mu$ m. The oxygen-permeation data reported next were measured on these membranes with about a 2–3- $\mu$ m-thick dense YSZ layer. More detailed microstructure of the YSZ/Pd composite (dual-phase) layer will be discussed later after presentation of oxygen-permeation data.

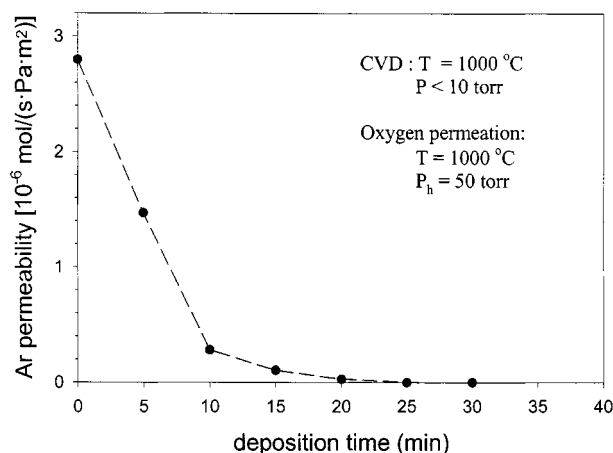


Figure 4. Ar permeability with deposition time.

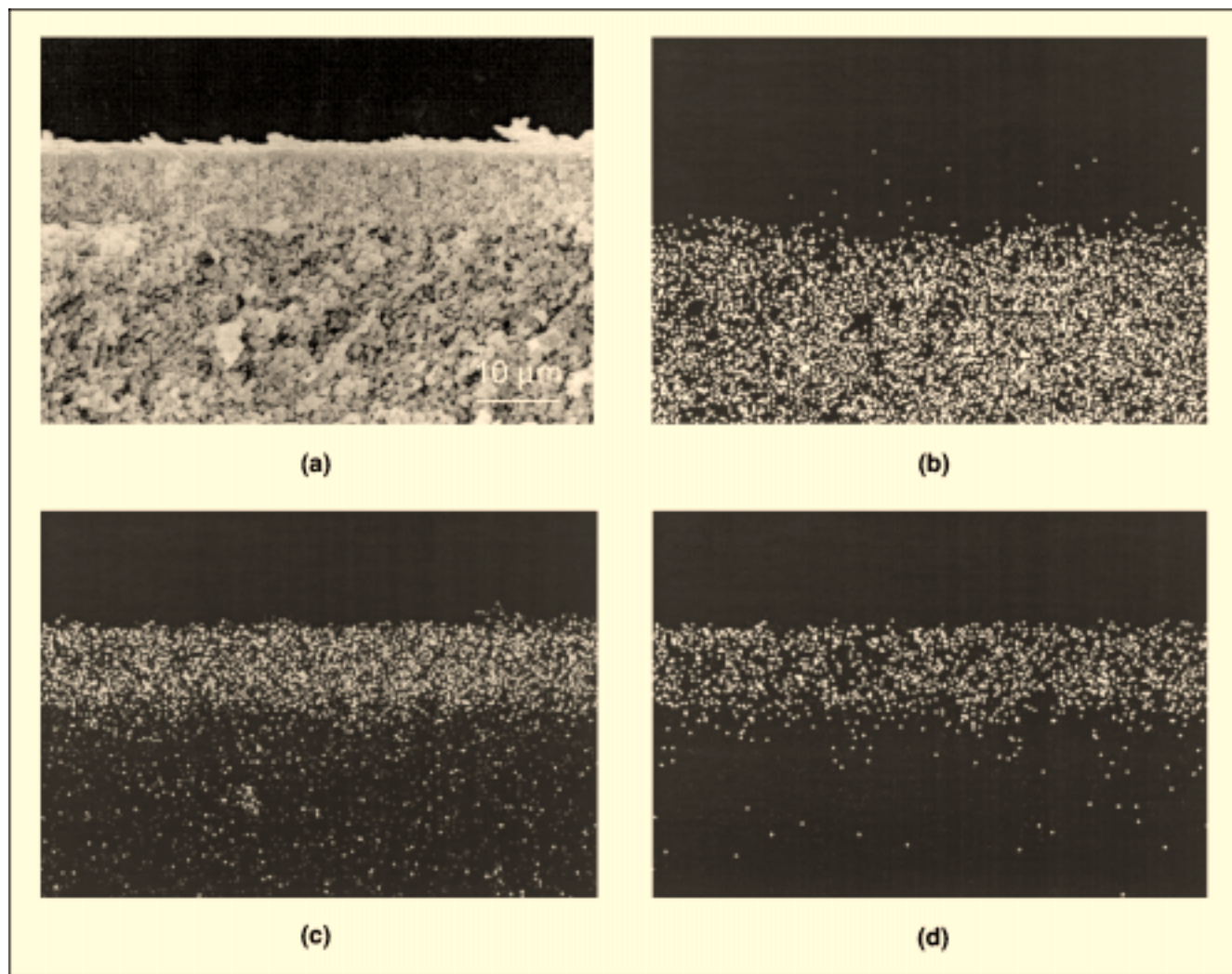


Figure 5. SEM photographs of YSZ/Pd composite (dual-phase) membrane: (a) SE image; (b) EDS mapping of Al; (c) EDS mapping of Zr; and (d) EDS mapping of Pd.

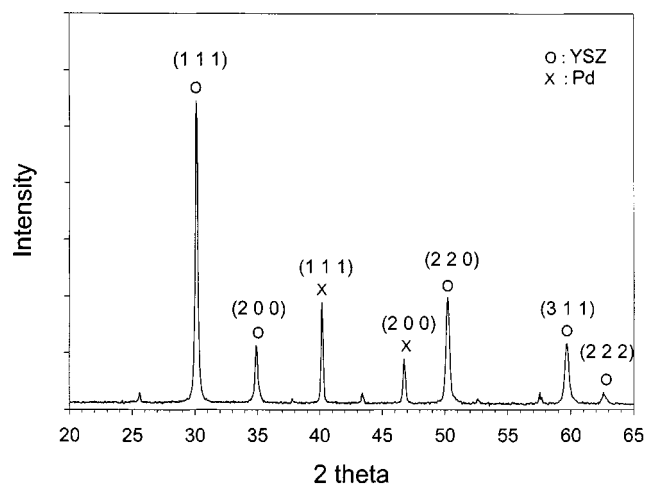


Figure 6. XRD pattern of YSZ/Pd composite (dual-phase) membrane.

### Oxygen permeation

The gas tightness of the membranes was checked by an *in situ* Ar-permeation experiment before and after deposition in the CVD reactor. The Ar permeation flux for most of membranes was reduced by a factor of 50–500 after the CVD pro-

Table 2. Comparison of R Values with Deposition Time and Film Thickness

Sample No.	Deposition Time [min]	Est. Film Thickness [ $\mu\text{m}$ ]	$I_{\text{PD}(111)}/I_{\text{YSZ}(111)}^*$
E-1114	15	0.4	37.4
E-0717	30	0.7	35.6
E-0618	30	1.1	34.9
E-1112	60	2.1	19.5
E-1120	60	2.5	17.3
E-1117	80	3.0	17.8

\* Before CVD/EVD,  $I_{\text{PD}(111)}/I_{\text{YSZ}(111)} \approx 43.3 \pm 2$ .

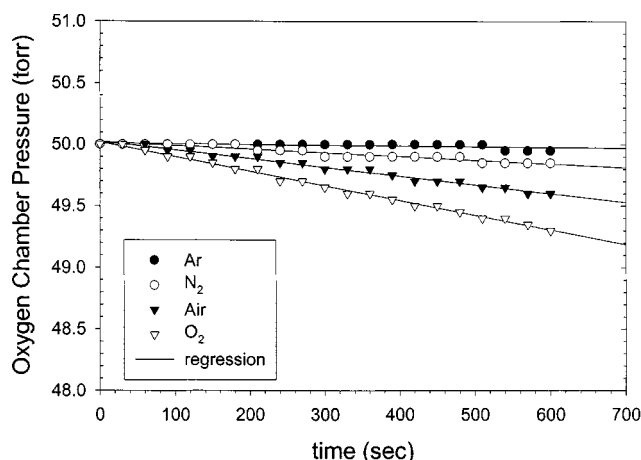
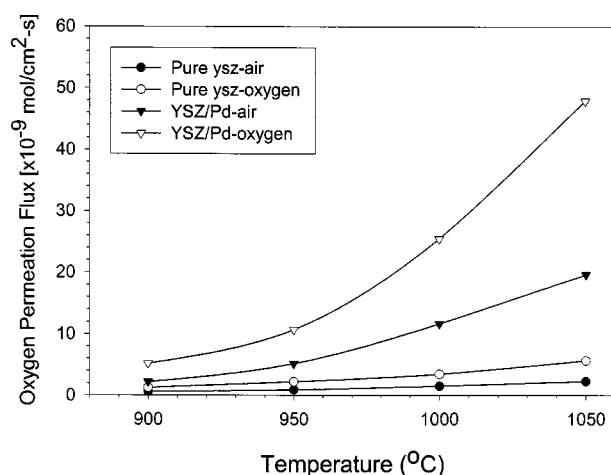


Figure 7. Pressure change in oxygen chamber in gas-permeation experiment.

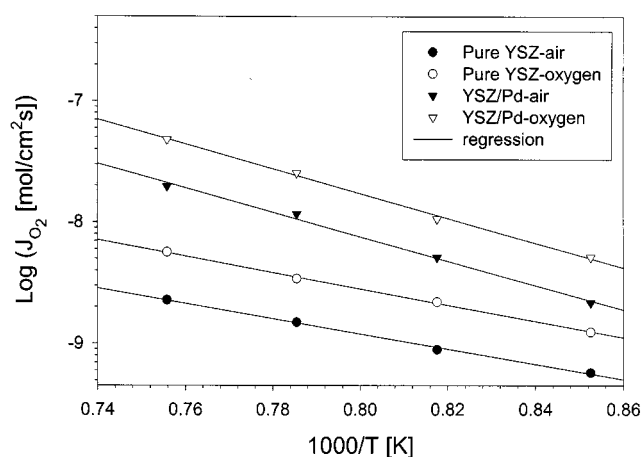
cess. A room temperature Ar-permeation experiment performed in a gas-permeation cell with O-ring seals showed much more permeation flux reduction (by a factor of up to 3000) for most membranes prepared by the CVD technique. This indicates that the high-temperature cement used for sealing the substrate in the CVD reactor was not completely gas tight in some cases. Since these defects on the cement allowed gases to permeate during the oxygen-permeation experiment, the leakage flow through the cement defects was estimated by separate Ar- and  $N_2$ -permeation experiments.

Figure 7 shows an example of pressure change in the oxygen-source chamber vs. time during *in situ* permeation experiments with Ar,  $N_2$ , air, and oxygen performed after deposition. The permeation flux could be calculated from the slopes of the pressure-change data vs. time by a simple mass balance equation. Oxygen leakage through the cement was corrected using Ar- and  $N_2$ -permeation data. In most cases, the ratio of  $J_{Ar}/J_{N_2}$  measured was approximately the same as the Knudsen factor, 1.43. Therefore, the leakage flow through the cement was determined by the Knudsen diffusion. Thus, the oxygen permeation flux through the dense membrane was calculated from the slope of pressure vs. time data with correction of leakage flow through the cement using the Ar- and  $N_2$ -permeation data. The leakage flux in most cases is less than 25% of the total oxygen flux measured. The accuracy of the measured oxygen-permeation flux is within  $\pm 20\%$  considering error propagation.

Oxygen-permeation fluxes through the YSZ/Pd composite (dual-phase) membranes were measured in the temperature 900–1050°C range. Figure 8a shows the oxygen-permeation fluxes through composite membranes vs. temperature. The oxygen-permeation fluxes through these membranes are in the range of  $2.18 \times 10^{-9}$ – $1.97 \times 10^{-8}$  mol/cm<sup>2</sup>·s and  $5.18 \times 10^{-9}$ – $4.79 \times 10^{-8}$  mol/cm<sup>2</sup>·s when air and oxygen are used as the permeate gases, respectively. During the oxygen-permeation experiment, the upstream and downstream oxygen partial pressures were maintained in the range of  $6 \times 10^{-3}$ – $2 \times 10^{-2}$  atm and  $1 \times 10^{-5}$ – $2 \times 10^{-4}$  atm, respectively. The oxygen permeation flux with oxygen as the permeate gas is about two times that with air as the permeate gas. Figure 8b shows Arrhenius plots of oxygen-permeation fluxes through



(a)



(b)

Figure 8. (a) Comparison of oxygen permeation flux through pure YSZ and YSZ/Pd composite (dual-phase) membranes; (b) Arrhenius plot of oxygen permeation flux through pure YSZ and YSZ/Pd composite (dual-phase) membranes.

YSZ/Pd composite (dual-phase) membranes. The data show the same activation energy of 193 kJ/mol for oxygen permeation with air or oxygen as the permeate gas.

In Figure 8, the oxygen-permeation fluxes of pure YSZ membranes prepared by CVD are compared with those of the YSZ/Pd composite (dual-phase) membranes. These pure YSZ membranes were on the same YSZ substrate and prepared under identical CVD conditions, except that no Pd was coated. Therefore, the dense layer of the YSZ membranes should be similar to that of the YSZ/Pd dual-phase membranes. As shown in Figures 8, the oxygen-permeation flux through YSZ/Pd dual-phase membranes was about 10 times higher than that of pure YSZ membranes. The Arrhenius plots show again the same activation energies for oxygen permeation through the pure YSZ membranes with both air or oxygen as the permeate gas, at a value of 124 kJ/mol. This activation energy is significantly lower than that for YSZ/Pd dual-phase membranes.

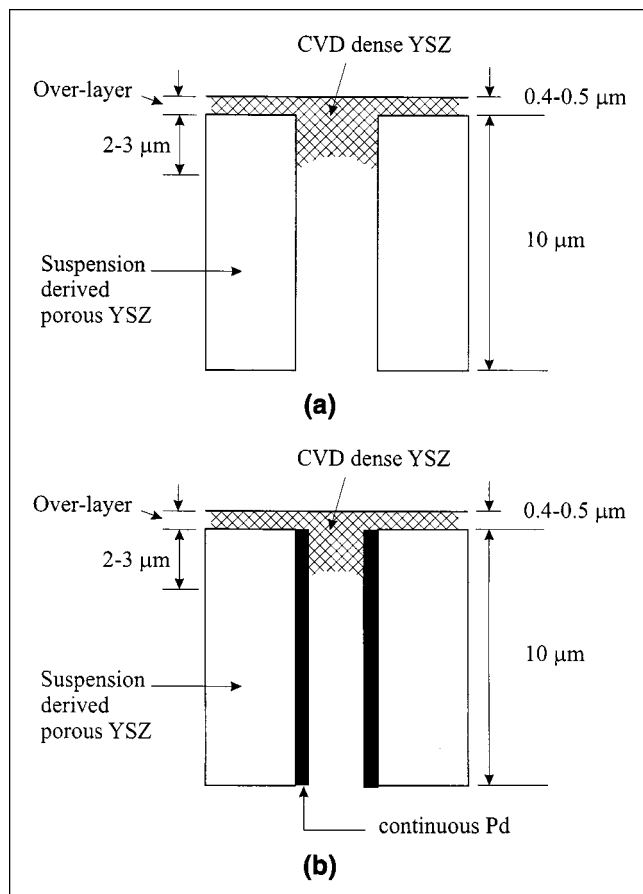


Figure 9. (a) Microstructure of pure YSZ membrane; (b) microstructure of YSZ/Pd composite (dual-phase) membrane.

Oxygen permeation through a thin pure YSZ membrane is determined by electronic conductivity of the bulk film and surface-charge-transfer reactions (Lin et al., 1992; Han et al., 1997). A possible microstructure of the present YSZ membrane is illustrated in Figure 9a. The dense YSZ formed by the CVD step includes a part inside the pore and a thin overlayer covering the surface of the suspension-derived porous YSZ. The oxygen-permeation resistance lies on the dense YSZ layer formed by CVD. Since this dense YSZ layer is less than 3 μm, both surface reaction and bulk electronic diffusion resistances are important (Han et al., 1997). Therefore, the apparent activation energy observed for oxygen permeation through the present YSZ membranes is an average of the activation energy for electron transport and surface reactions.

For a true thin dual-phase YSZ/Pd membrane, the bulk electronic transport resistance is negligible and the oxygen permeation flux is determined by the ionic conductivity of the bulk YSZ film, which is several orders of magnitude higher than its electronic conductivity. In this case, one would expect an oxygen-permeation flux for the YSZ/Pd dual membrane of about several orders of magnitude higher than that for the pure YSZ membrane if the mass-transfer resistances of other steps can be neglected. The present results show

oxygen permeation flux for the YSZ/Pd composite (dual-phase) membrane of about 10 times that for the pure YSZ membrane. These results can be explained if the microstructure for the pure YSZ membrane shown in Figure 9a is accepted and applied to the YSZ/Pd composite membrane.

Figure 9b shows the microstructure of the YSZ/Pd composite (dual-phase) membrane. The amount of YSZ deposited inside the pores of the YSZ/Pd layer forms a truly dual-phase membrane with negligible resistance for oxygen permeation. The surface reaction and electronic transport resistances of the thin dense YSZ overlayer on the surface of the YSZ/Pd layer control the rate of oxygen permeation. This dense YSZ overlayer, possibly of about 0.3 to 0.5 μm in thickness, is much thinner than the total dense YSZ layer (about 3 μm) in the pure YSZ membrane shown in Figure 9a. The smaller resistance of electron transport in the thinner YSZ overlayer of YSZ/Pd composite (dual-phase) membranes (Figure 9b) results in a higher oxygen-permeation flux as compared to the pure YSZ membrane shown in Figure 9a. Furthermore, the thinner film increases the relative importance of the resistance of the surface reaction, which usually has a larger activation energy than that for the bulk-diffusion step for oxygen permeation (Lin et al., 1994). This explains the higher apparent activation energy for oxygen permeation for the YSZ/Pd composite (dual-phase) membranes than that for pure YSZ membrane.

## Conclusions

Gas-tight thin YSZ/Pd composite (dual-phase) membranes can be fabricated by a technique that combines liquid-phase coating and CVD methods. The YSZ/Pd composite (dual-phase) membranes consist of a dual-phase dense YSZ/Pd layer of 2–3 μm in thickness and a submicron-thick dense YSZ overlayer. Oxygen permeation fluxes through the YSZ/Pd composite (dual-phase) membranes were investigated *in situ* in the CVD reactor, which avoided possible high-temperature sealing problems. The oxygen-permeation fluxes through these YSZ/Pd composite (dual-phase) membranes are in the  $2 \times 10^{-9}$  to  $5 \times 10^{-8}$  mol/cm<sup>2</sup>·s range, about one order of magnitude higher than pure YSZ membranes prepared in similar conditions. The apparent activation energies for oxygen permeation in the 900–1,050°C temperature range are 193 kJ/mol for the YSZ/Pd composite (dual-phase) membranes and 124 kJ/mol for pure YSZ membranes. Highly oxygen-permeable thin dual-phase YSZ/Pd membranes could be obtained if the growth of the dense YSZ overlayer is avoided.

## Acknowledgment

The authors are grateful for the financial support on this project from the National Science Foundation (Career Award: CTS-9502437).

## Literature Cited

- Arashi, H., and H. Naito, "Oxygen Permeability in ZrO<sub>2</sub>-TiO<sub>2</sub>-Y<sub>2</sub>O<sub>3</sub> System," *Solid State Ionics*, **53-56**, 431 (1992).
- Barin, I., *Thermochemical Data of Pure Substances*, 3rd ed., Weinheim, New York (1995).
- Barin, I., and O. Knacke, *Thermochemical Properties of Inorganic Substances*, Springer-Verlag, Berlin (1973).
- Bouwmeester, H. J. M., H. Kruidhof, and A. J. Burggraaf, "Importance of the Surface Exchange Kinetics as Rate Limiting Step in



- Oxygen Permeation Through Mixed-Conduction Oxides," *Solid State Ionics*, **72**, 185 (1994).
- Brinkman, H. W., H. Kruidhof, and A. J. Burggraaf, "Mixed Conducting Yttrium-Barium-Cobalt-Oxide for High Oxygen Permeation," *Solid State Ionics*, **68**, 173 (1994).
- Chen, C. S., H. Kruidhof, H. J. M. Bouwmeester, H. Verweij, and A. J. Burggraaf, "Oxygen Permeation Through Oxygen Ion Oxide-Noble Metal Dual-Phase Composites," *Solid State Ionics*, **86-88**, 569 (1996).
- Chen, C. S., B. A. Boukamp, H. J. M. Bouwmeester, G. Z. Cao, H. Kruidhof, A. J. A. Winnubst, and A. J. Burggraaf, "Microstructural Development, Electrical Properties and Oxygen Permeation of Zirconia-Palladium Composites," *Solid State Ionics*, **76**, 23 (1995).
- Cullity, B. D., *Elements of X-Ray Diffraction*, Addison-Wesley, Reading, MA (1978).
- Han, J., G. Xomeritakis, and Y. S. Lin, "Oxygen Permeation Through Thin Zirconia/Yttria Membranes Prepared by EVD," *Solid State Ionics*, **93**, 263 (1997).
- Han, P., and W. L. Worrell, "Mixed (Oxygen Ion and *p*-Type) Conductivity in Yttria-Stabilized Zirconia Containing Terbium," *J. Electrochem. Soc.*, **142**, 4235 (1995).
- Jankowski, A. F., and J. P. Hayes, "Sputter Deposition of Yttria-Stabilized Zirconia onto a Porous Au Substrate," *J. Vac. Sci. Technol.*, **13**, 658 (1995).
- Kim, J., and Y. S. Lin, "Synthesis and Characterization of Suspension-Derived, Porous Ion-Conducting Ceramic Membranes," *J. Amer. Ceram. Soc.*, **82**, 2641 (1999).
- Lin, Y. S., K. J. de Vries, H. W. Brinkman, and A. J. Burggraaf, "Oxygen Semipermeable Solid Oxide Membrane Composites Prepared by Electrochemical Vapor Deposition," *J. Memb. Sci.*, **66**, 211 (1992).
- Lin, Y. S., W. Wang, and J. Han, "Oxygen Permeation Through Dense Mixed-Conducting Oxide Membranes," *AIChE J.*, **40**, 786 (1994).
- Mazanec, T. J., T. L. Cable, and J. G. Frye, "Electrocatalytic Cells for Chemical Reaction," *Solid State Ionics*, **53-56**, 111 (1992).
- Nigara, Y., J. Mizusaki, and M. Ishigame, "Measurement of Oxygen Permeability in CeO<sub>2</sub> Doped CSZ," *Solid State Ionics*, **79**, 208 (1995).
- Park, J. H., and R. N. Blumenthal, "Electronic Transport in 8 Mol Percent Y<sub>2</sub>O<sub>3</sub>-ZrO<sub>2</sub>," *J. Electrochem. Soc.*, **136**, 2867 (1989).
- Pei, S., M. S. Kleefisch, T. P. Kobylinski, J. Faber, C. A. Udovich, V. Zhang-McCoy, B. Dabrowski, U. Balachandran, R. L. Mieville, and R. B. Poeppel, "Failure Mechanism of Ceramic Membrane Reactors in Partial Oxidation of Methane to Synthesis Gas," *Catal. Lett.*, **30**, 201 (1995).
- Qi, X., and Y. S. Lin, "Electrical Conducting Properties of Proton-Conducting Terbium-Doped Strontium Cerate Membrane," *Solid State Ionics*, **120**, 85 (1999).
- Shen, Y. S., M. Liu, D. Taylor, S. Bolagopal, A. Joshi, and K. Krist, "Mixed Ionic-Electronic Conductors Based on Bi-Y-O-Ag Metal-Ceramic System," *Proc. Int. Symp. on Ionic and Mixed Conducting Ceramics*, Vol. 94-12, T. A. Ramanarayanan et al., eds., The Electrochemical Society, NJ, p. 574, (1994).
- Uhlhorn, R. J. R., V. T. Zaspalis, K. Keizer, and A. J. Burggraaf, "Synthesis of Ceramic Membranes Part II Modification of Alumina Thin Films: Reservoir Method," *J. Mater. Sci.*, **27**, 538 (1992).
- Wang, L. S., and S. A. Barnett, "Sputtering Deposited Medium-Temperature Solid Oxide Fuel Cells with Multilayer Electrolytes," *Solid State Ionics*, **61**, 273 (1993).
- Zeng, Y., Y. S. Lin, and S. L. Swartz, "Perovskite-Type Ceramic Membrane: Synthesis, Oxygen Permeation and Membrane Reactor Performance for Oxidative Coupling of Methane," *J. Memb. Sci.*, **150**, 87 (1998).

Manuscript received Aug. 27, 1999, and revision received Feb. 29, 2000.